JOURNAL OF AIRCRAFT
Vol. 38, No. 2, March–April 2001

Exhaust Ducting Effects on Takeoff Lift Loss of Two-Dimensional Hypersonic Configuration

Robert E. Bond,* Gary J. Morris,† and John L. Loth‡
West Virginia University, Morgantown, West Virginia 26506-6106

The National Aerospace Plane (NASP) configuration was designed to suit propulsion needs at hypersonic speeds. Like many hypersonic configurations, its lower fuselage surface was shaped to suit the propulsion system with an oblique shock compression ramp, scramjet combustion module, and a single expansion ramp nozzle. To minimize drag, the nose was very thin and the upper surface nearly flat. Previous work has shown this configuration produces poor low-speed and in-ground effect performance. This is characterized by significant power-on lift reduction that is intensified by ejector action while in-ground effect. The effects of exhaust ducting on the ground effect lift coefficients and surface pressure distributions of a two-dimensional model based on the NASP fuselage centerline geometry are demonstrated. A two-dimensional configuration was used in an attempt to separate the complex three-dimensional effects from the key problems with this configuration.

Nomenclature

A_p^*	=	ejector primary choked flow area
A_s	=	ejector secondary flow area
b	=	three-dimensional model wing span
C_L	=	three-dimensional lift coefficient, lift/$q_\infty S$
C_l	=	two-dimensional lift coefficient
C_p	=	pressure coefficient
C_T	=	three-dimensional thrust coefficient
C_t	=	two-dimensional thrust coefficient
c	=	two-dimensional model length, referenced to as chord length
h	=	model height above ground plane, in.
h/b	=	nondimensional model height above ground plane (three-dimensional models)
h/c	=	nondimensional model height above ground plane (two-dimensional model)
q_∞	=	tunnel dynamic pressure, in. H_2O or psi
Re	=	Reynolds number
S	=	three-dimensional model planform area including both wing and fuselage areas
T	=	static thrust along waterline, lbf
x/c	=	nondimensional chord position
α	=	angle of attack, deg

Introduction

A SIGNIFICANT amount of work has been performed to investigate the takeoff/ground effect characteristics of basic hypersonic configurations. As a result of this work, a significant aerodynamic problem was revealed where hypersonic configurations exhibit significant lift loss characteristics when operating in close ground proximity, with power-on. The following is a summary of previous work performed to define the low-speed ground effect characteristics.

Models used for research in this area have all used an array of high-pressure ejectors positioned inside the engine nacelle to simulate engine inlet flow as well as thrust from high exhaust velocity. The thrust coefficient C_T was defined by normalizing the static model thrust divided by the tunnel dynamic pressure and entire model planform area, including wing and fuselage areas. Lift-off thrust values were defined by $C_T = 0.4$.

Preliminary research in this field was conducted by Gatlin[1,2] at NASA Langley Research Center. Gatlin used a generic hypersonic configuration (GHC) model with an overall length of 2.867 m (9.408 ft) mounted in the NASA Langley Research Center 14 × 22 ft subsonic tunnel, as shown in Fig. 1. Tests were run at thrust coefficients from 0.0 to 0.8 and at a unit Reynolds number of 1.3×10^6/ft. Ground effect data were taken for a takeoff, and approach representative angle of attack chosen to be $\alpha = 12$ deg. Gatlin performed tests to determine the effect of the model height and thrust coefficient on the base configuration lift, drag, and pitching moment. With respect to the lift coefficient data obtained for the base geometry GHC, Gatlin[1] noted that "These data indicate conventional ground effects for the power-off condition as illustrated by increased lift with decreasing model height above the floor. However, this trend reversed as thrust was increased and significant lift losses developed as the model was lowered into ground effect." This power-on, ground effect lift loss generated at takeoff conditions is illustrated by the base configuration data presented in Fig. 2.

In an attempt to obtain flow separation on the single expansion ramp nozzle (SERN) of the GHC, Gatlin[1] tested various flow deflector strips. These strips ranged from 0.375 to 3 in. tall, spanned the entire width of engine simulation system, and placed on the SERN just downstream of the engine exhaust. As a result of these tests, it was discovered that the flow simply jumped the smaller deflector strips and remained attached to the SERN; however, for the larger strips, the flow was successfully separated. In addition to these strips, various wedges from 14 to 45 deg were attached to the SERN (Fig. 1). The lift coefficient data obtained from the most effective modifications are shown in Fig. 2. Based on Fig. 2, it is evident that the use of these devices can not only reverse the ground effect lift loss, but can also significantly increase the overall lift coefficient by deflecting the exhaust vector down to achieve a lift component. Although these modifications showed marked improvements in lift coefficient, they imposed tremendous drag penalties. These drag increases ranged from $\Delta C_D = 0.015$ for the 30-deg wedge to $\Delta C_D = 0.15$ for the 45-deg wedges.

Further investigation into the ground effect characteristics of hypersonic configurations was performed by Gatlin and Kjerstad.[3] They used a 2.9-m- (9.5-ft) long (6.5% scale) model of the National Aerospace Plane (NASP) test technique demonstrator (TTD) concept. This model (Fig. 3) was a more accurate representation of a NASP configuration compared to the GHC and was

Received 20 May 1999; revision received 1 October 1999; accepted for publication 11 October 1999.

*Research Assistant Professor, Department of Mechanical and Aerospace Engineering, College of Engineering and Mineral Resources. Member AIAA.

†Professor, Department of Mechanical and Aerospace Engineering, College of Engineering and Mineral Resources. Member AIAA.

‡Professor, Department of Mechanical and Aerospace Engineering, College of Engineering and Mineral Resources. Member AIAA.

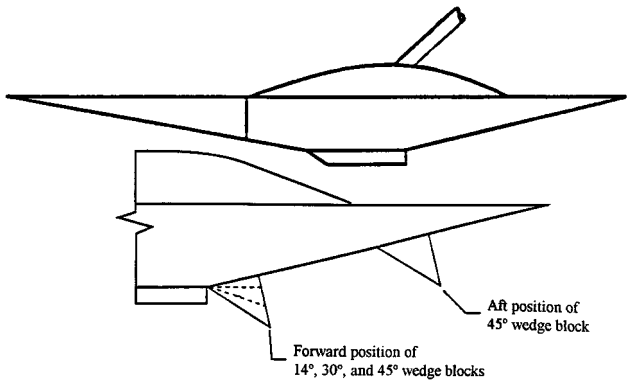

Fig. 1 Generic hypersonic configuration and relative position of flow deflector wedge blocks.[2]

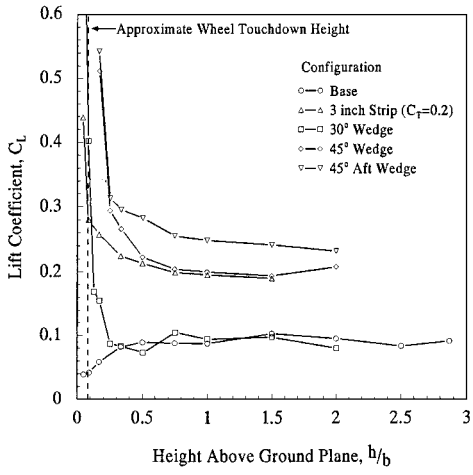

Fig. 2 Effect of h/b on C_L for GHC[2] (α = 12 deg and C_T = 0.4, various geometries).

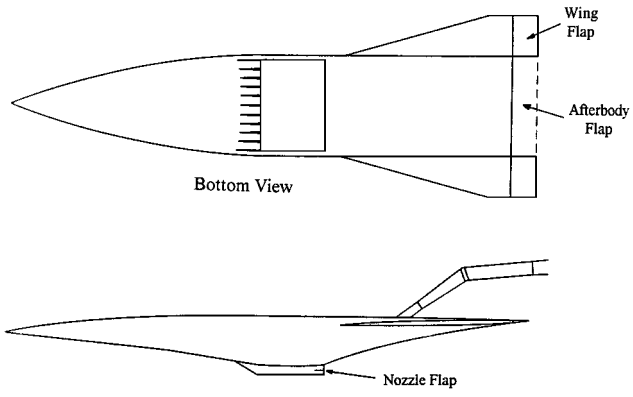

Fig. 3 NASP test technique demonstrator showing position of afterbody flap and nozzle flap.[3]

equipped with movable control surfaces, which included an afterbody flap and a nozzle flap (Fig. 3), located in the engine nacelle near the exhaust plane. These two surfaces were used to study their effect on the ground effect characteristics of the TDD. This model was tested in the NASA Langley Research Center 14×22 ft subsonic tunnel over an angle of attack range of from -1 to 27 deg. The freestream dynamic pressure q_∞ and thrust coefficient C_T ranged from 10 to 80 psf and from 0.0 to 0.8, respectively, although most data were taken with $q_\infty = 40$ psf with a corresponding Reynolds number of 1.2×10^6/ft. The ground effect characteristics for the base TTD geometry were obtained by the use of a fixed ground plane. Most of the ground effect data were obtained at the liftoff representative angle of attack of 10 deg. These data in-

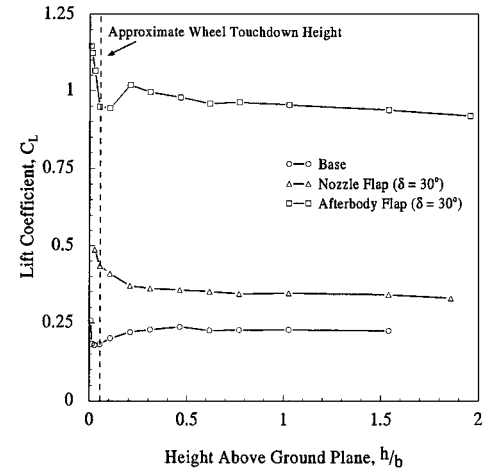

Fig. 4 Effect of h/b on C_L for NASP TTD[3] (α = 10 deg and C_T = 0.4, various geometries).

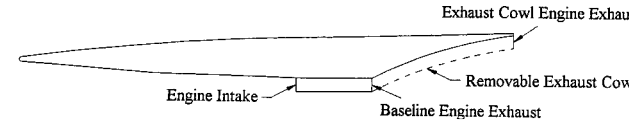

Fig. 5 NASP display version 2 showing removable exhaust cowl.[4]

cluded the lift, drag, and moment coefficients as a function of model height.

Selected ground effect lift coefficient data are shown in Fig. 4. From these data, it can be seen that the NASP TTD base configuration ground effect data follow the same trend as those for the GHC when operating at liftoff conditions. Also shown in Fig. 4 are the data obtained with either the nozzle flap or the afterbody flap deflected 30 deg. When the nozzle flap was used, the ground effect lift loss reversed to a lift increase with reducing ground spacing. In addition to this, there was a freestream lift coefficient increase of approximately 0.1. When the afterbody flap was used, an initial increase in lift coefficient with reducing ground spacing reversed to a significant lift loss as touchdown height was approached. The use of this flap increased the freestream lift coefficient by approximately 0.7, to approximately four times the base lift coefficient. However, associated with these lift coefficient increases came significantly increased drag. Drag coefficients for the nozzle flap were increased by approximately 0.125, and when the afterbody flap was used, they increased by in excess of 0.3. In addition, the afterbody flap had large effects on the pitching moment coefficient, lending it more use as a pitch control device than for ground effect lift coefficient improvements.

The final work that will be discussed here is that of Smith[4] and Smith et al.[5] at West Virginia University (WVU). They investigated a model with an overall length of 1.52 m (5 ft), based on the NASP display model version 2 with a removable exhaust cowl (Fig. 5), mounted in the WVU 6×4 ft low-speed tunnel. Figure 6 shows ground effect lift coefficient data taken for this model operating at takeoff representative conditions of $\alpha = 10$ deg and thrust coefficient $C_T = 0.4$. Also shown in Fig. 6 are the data obtained for the maximum test thrust coefficient of $C_T = 0.6$. When the baseline data were considered, it was noted that the lift coefficient initially increased as the model was lowered from h/b of 2 to 0.5; however, when the model was lowered still further, this trend reversed and there was a significant decrease in lift coefficient. When the exhaust cowl was added, which effectively moved the engine exhaust plane to the aft end of the model, the ground effect lift loss, in near ground proximity, was reversed. Additionally, the use of this modification increased the freestream lift coefficient at takeoff thrust by approximately 0.21, or 63%. Similar to the other modifications tested, there was a drag penalty associated with this system. However, in this case the penalty was much smaller with an increase of only $\Delta C_D = 0.05$

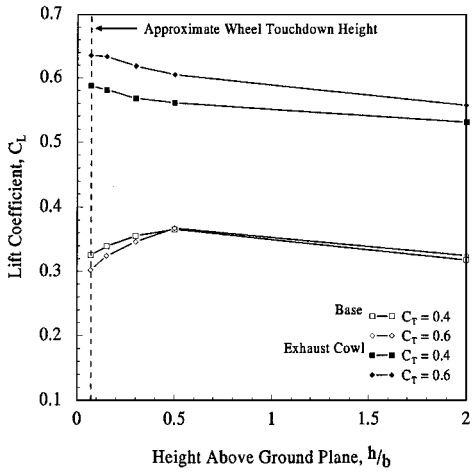

Fig. 6 Effect of h/b on C_L for display NASP configurations[4] ($\alpha = 10$ deg, various geometries).

Fig. 7 Cross section of two-dimensional NASP model including pressure tap locations.

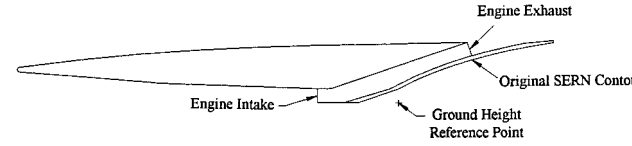

a) Internal exhaust ducting

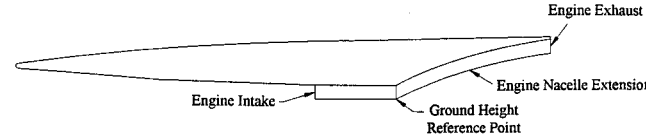

b) External exhaust ducting

Fig. 8 Two-dimensional NASP model exhaust ducting techniques.

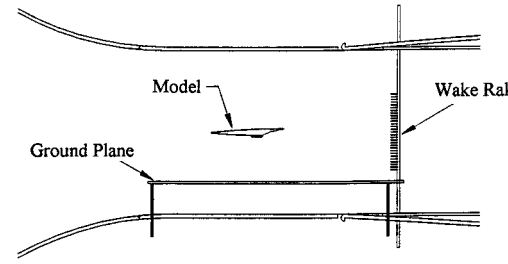

Fig. 9 Wind-tunnel test section including model, ground plane, and wake rake.

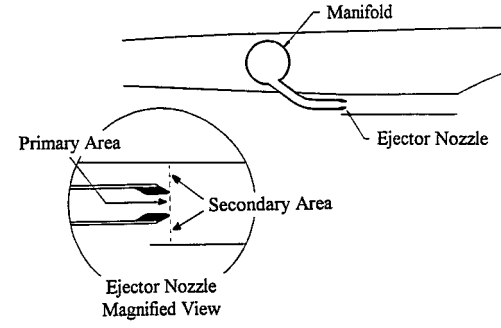

Fig. 10 Model cross section showing ejector system and flow areas.

when compared to the techniques that produced significantly more lift.

The purpose of the present investigation is to determine how exhaust ducting techniques when applied to the NASP affect the ground effect lift loss characteristics. The three-dimensional nature of the models previously tested complicates the flowfield and makes it harder to determine what effect the exhaust ducting has on overall pressure distribution on the surface of the NASP. Therefore, it was decided to test a two-dimensional model based on the centerline cross section of the NASP display model version 2. This model provides a detailed surface pressure distribution with a reasonable number of pressure taps and correlation with two-dimensional computational fluid dynamics (CFD) model flowfield predictions. The flow entrainment and separation zones clearly demonstrate the influence the NASP fuselage geometry and exhaust ducting have on the observed ground effect performance.

Experimental Apparatus

The basis for the model that was used for this research was the NASP display model version 2 (Ref. 6). The cross section of the two-dimensional model (Fig. 7) was based on the centerline dimensions of this configuration. The wind-tunnel model was designed with a chord length of 50.8 cm (20 in.) and a span of 81.3 cm (32 in.). This allowed the model to span completely the available wind-tunnel test section to simulate two-dimensional flow.

In addition, two modifications of the base configuration were tested. They are 1) the internal duct where the exhaust was routed through an internal duct as shown in Fig. 8a and 2) the external duct where the flow is directed along the original SERN through the use of an engine nacelle extension (Fig. 8b).

The location of the ground height reference point is shown for each configuration in Figs. 7 and 8. This point is located at the point of closest ground proximity for the base configuration and remains in the same body-fixed coordinates for the internal and external ducting configurations.

Experimental tests were run using these models in the WVU (32×45 in.) subsonic wind tunnel (Fig. 9). Data were taken at a dynamic pressure of 311 Pa (6.5 psf), which yielded $Re = 7.25 \times 10^5$ based on the model chord. The average freestream turbulence intensity when operating under these conditions was found to be 0.215%, with a standard deviation of 0.075 as measured using a hot-film anemometer in the empty test section. With this model, with the ground plane removed, the tunnel blockage was found to be 8.4% at a 10-deg angle of attack. This blockage was calculated based on the model frontal area and does not account for boundary-layer development on the test section walls.

Model thrust was produced by using a high-pressure ejector system located in the model nacelle (Fig. 10). This system was powered by 32 choked nozzles with throat diameters of 3.2 mm (0.126 in.). These nozzles were located at the inlet of the nacelle, which was used as a constant area mixing chamber. Based on this geometry, the ejector system had a secondary to primary area ratio of $A_s/A_p^* = 40.8$. Similar to the previously tested three-dimensional configuration, the static thrust levels produced by this system were used in the determination of the operational thrust coefficient as given by Eq. (1):

$$C_t = (T/\text{span})_{\text{static}}/q_\infty c \tag{1}$$

Normal and pitching moment coefficients were calculated from model static pressure distributions. These distributions were obtained by measuring the static pressure at 89 independent static pressure taps placed along the model centerline. To minimize the error associated with approximating the continuous pressure distribution with measurements at discrete points, these taps were placed based on a CFD predicted representative pressure distribution, as shown in Fig. 11. The resulting pressure tap locations are shown in Fig. 7. These CFD results were generated using FLUENT version

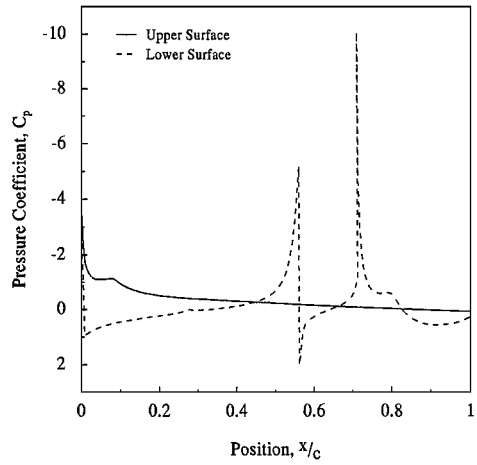

Fig. 11 CFD predicted surface C_p data (α = 10 deg and C_t = 0.4).

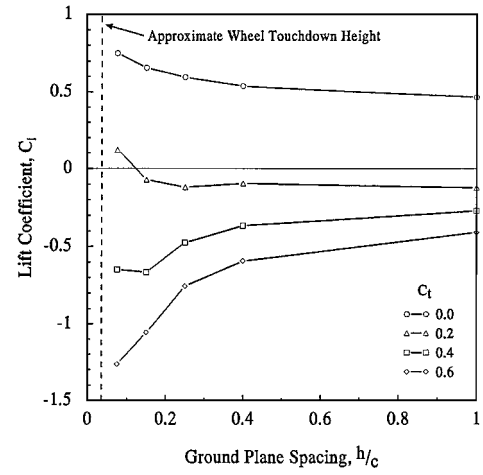

Fig. 12 Effect of ground plane spacing on lift coefficient, two-dimensional base configuration, α = 10 deg.

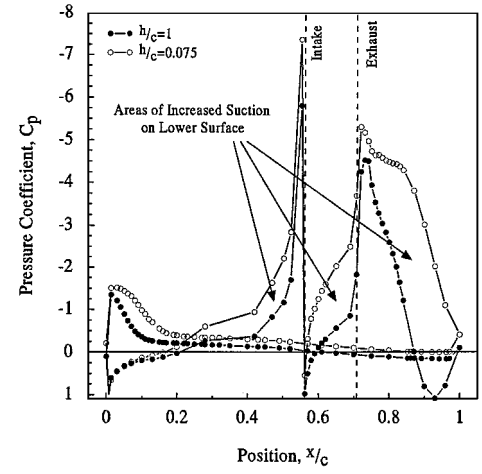

Fig. 13 Comparison of C_p distribution for h/c = 1 and 0.075, base configuration, α = 10 deg and C_t = 0.6.

4.32 with a 25,000 cell grid and, when compared to the experimental results, were found to be in reasonable agreement.

Ground effect data were taken by the use of a variable position ground plane (see Fig. 9) with an overall length of 1.83 m (6 ft). The ground plane spacing was varied by moving the ground plane nearer or farther from the model through the use of four screw jacks. Out-of-ground effect data were taken with the ground plane removed from the test section to minimize wall effects. Because of the complicated aerodynamic interaction between the boundary layer developed on this ground plane and the model, no attempt was made to remove its effect.

Experimental Results

The objective of this research was to characterize the effect of exhaust ducting on the ground effect aerodynamics of a two-dimensional model of the NASP with thrust simulation.

The results of this investigation were all obtained at the maximum practical Reynolds number of approximately 7.25×10^5, based on the model chord, and were obtained with no artificial boundary-layer tripping of any form. This value closely approximates the Reynolds numbers used in the literature; however, it is orders of magnitude lower than the Reynolds number at which the proposed NASP would operate. Because of this, these results should not be considered exactly representative of expected results from full-scale three-dimensional flight hardware.

The coefficients reported and graphically displayed in the following sections are measured and computed data and apply only to the two-dimensional hypersonic model tested. They are not directly applicable to actual expected flight conditions. To approximate more closely free-flight data, these data should be corrected for Reynolds number and tunnel blockage effects using the procedure outlined by Allen and Vincenti[7] or its equivalent. Although this was not performed for this paper, these corrections are expected to change the data by less than 10%. The total uncertainty of the lift coefficient data presented in the Figs. 14 and 16 is 7.1% or on the order of the symbol size used in the figures. The pressure coefficient data is of greater accuracy than represented by the symbol sizes with an error of 3.8%.

Ground effect data were obtained at a liftoff representative angle of attack of 10 deg, which corresponded with the related studies noted in the literature. The liftoff representative thrust coefficient was defined to be $C_t = 0.4$; however, data are presented over a range of thrust coefficients from 0.0 to 0.6.

Base Configuration

The base configuration lift coefficient data were plotted as a function of the nondimensional ground plane spacing in Fig. 12. In Fig. 12, the out-of-ground effect data are represented at $h/c = 1$, which was the approximate spacing between the model and the test section wall. For thrust coefficients of 0.0 and 0.2, the effect of lowering the model into ground effect acts to increase the lift coefficient. At thrust coefficients in excess of 0.2, the ground effect characteristics changed markedly. For C_t values of 0.4 and 0.6, a strong lift loss was encountered as the model was lowered into ground effect. This was due to reduced static pressure on the lower surface caused by the increased ejector effect with reduced ground plane spacing. Where the model exhibited a lift increase of $\Delta C_l = 0.287$ when lowered into ground effect at zero thrust, it changed to a strong lift decrease of $\Delta C_l = -0.853$ at the maximum thrust coefficient of $C_t = 0.6$. This increased lift loss with increasing thrust coefficient was similar to that experienced for the three-dimensional models. At a thrust coefficient of 0.6, the lift coefficient for the two-dimensional model had a maximum change of 208%, from $C_l = -0.410$ at $h/c = 1$ to $C_l = -1.263$ at $h/c = 0.075$. When the thrust coefficient was reduced to 0.4, the maximum lift loss was 145% from the $h/c = 1$ to the $h/c = 0.15$ case.

To illustrate the effect of ground plane spacing on the model surface pressure distribution, Fig. 13 was constructed. Plotted in Fig. 13 are the data obtained at minimum and maximum ground plane spacings ($h/c = 0.075$ and 1) with the model operating at the maximum tested thrust coefficient ($C_t = 0.6$). From Fig. 13, the cause of the ground effect lift loss is readily identifiable. When the upper surface of the model is considered, it can be seen that close ground proximity is accompanied by a slight increase in upper surface suction, acting to increase the overall lift coefficient. However, the effect of ground plane spacing on the lower surface pressure distribution is far more dramatic. On this surface, three strong low-pressure regions are significantly enhanced when the model is in close ground

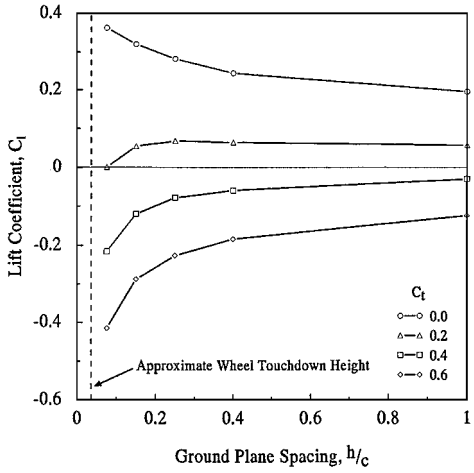

Fig. 14 Effect of ground plane spacing on lift coefficient, two-dimensional internal duct configuration, α = 10 deg.

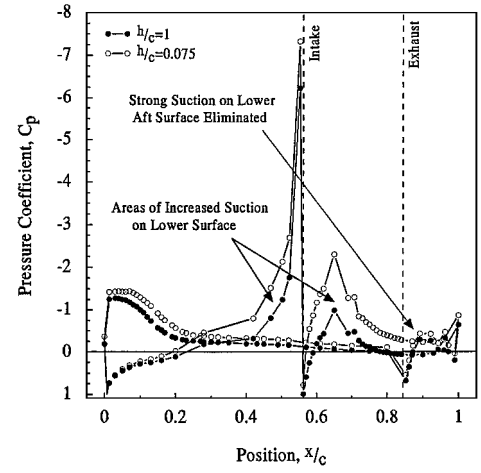

Fig. 15 Comparison of C_p distribution for h/c = 1 and 0.075, internal duct configuration, α = 10 deg and C_t = 0.6.

proximity. These regions are located just upstream of the engine intake, on the engine nacelle, with the primary region being located just downstream of the engine exhaust location. The combination of the strong suction regions formed on the lower surface overwhelms the sightly increased suction on the upper surface to reduce dramatically the overall section lift coefficient. Similar pressure distribution changes were noted at lower thrust coefficients and angles of attack where the ground effect lift loss characteristic was present.

Internal Duct Configuration

Ground effect lift coefficient characteristics for the internal duct configuration are shown in Fig. 14. These data show, for the zero-thrust case, the typical ground effect characteristic of increased lift coefficient with reduced ground plane spacing. However, when thrust is applied, this characteristic reverses, and the undesirable ground effect lift loss trends develop. Although this ground effect characteristic reversal develops at far lower thrust coefficients than for the base configuration, note that overall lift coefficient dependence on thrust coefficient is greatly reduced for the internal duct configuration. This is illustrated by the maximum reduction in lift coefficient produced at any given ground plane spacing by the application of maximum tested thrust. With the model in the out-of-ground effect position ($h/c = 1$) the change in lift coefficient from $C_t = 0.0$ to 0.6 is $\Delta C_l = -0.873$ for the base configuration, but only -0.319 for the internal duct configuration. When the model is in-ground effect at $h/c = 0.075$, these values change to -2.014 for the base configuration and -0.778 for the internal duct configuration. This reduced lift coefficient dependence on thrust level would produce an aircraft with much more forgiving flying qualities.

The effect of ground plane spacing on the surface pressure distribution for the internal duct configuration is illustrated in Fig. 15. Figure 15 contains data for the extreme ground effect spacings of $h/c = 1$ and 0.075 at the maximum thrust coefficient of $C_t = 0.6$. These data show a similar suction increase with reduction in ground spacing on the lower surfaces located upstream of the engine intake and on the engine nacelle. However, due to the exhaust exiting on the upper surface, thereby eliminating the ejector action below the model, the internal duct configuration shows no development of the strong suction region on the SERN experienced by the base configuration. It is the lack of this strong low-pressure region and that at $\alpha = 10$ deg the exhaust vector for this configuration is nearly parallel to the freestream that greatly reduces the effect of thrust on the section lift coefficient.

External Duct Configuration

The ground effect lift characteristics for the external duct configuration are shown in Fig. 16. Based on these data, it can be seen that this configuration produced much improved ground effect performance than either the base or the internal duct configurations. This configuration shows the typical ground effect characteristics for thrust coefficients of 0.0 and 0.2. At higher thrust levels, the undesired ground effect lift loss is still present; however, it is much less dramatic than for the other two configurations. If the maximum thrust coefficient case is considered at h/c values of 1 and 0.075, the base configuration shows a lift loss of $\Delta C_l = -0.854$, the internal duct configuration shows $\Delta C_l = -0.292$, and the external duct configuration only experiences a ΔC_l of -0.270. This is a 68% reduction in lift loss when compared to the base configuration. In addition to this improved ground effect performance, this configuration shows a second, and perhaps more significant, advantage of increased lift throughout the power-on regime. It is evident, from Fig. 16, that nearly all of the lift coefficient data for the external duct configuration are positive, lift-producing values. In fact, this is the only configuration tested that produces positive lift at the takeoff representative thrust coefficient of $C_t = 0.4$.

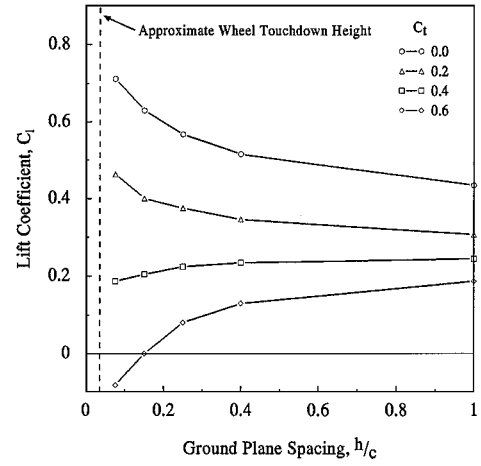

Fig. 16 Effect of ground plane spacing on lift coefficient two-dimensional external duct configuration, α = 10 deg.

When the pressure distributions both in- and out-of-ground effect are considered (Fig. 17) significant differences between the base and external duct configurations can be seen. Similar to the internal duct configuration, the external duct configuration shows a greatly reduced suction on the SERN portion of the lower surface due to reduced ejector action below the model. The external duct configuration upper surface shows a larger suction region on the forebody than for either the base or internal duct configurations. Finally, the external duct configuration experienced minimal suction increases on the surface upstream of the engine intake. These characteristics all combine to increase greatly the overall section lift coefficient and to reduce the ground effect lift loss characteristic.

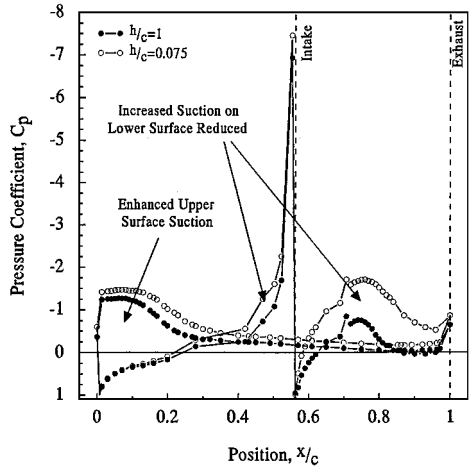

Fig. 17 Comparison of C_p distribution for h/c = 1 and 0.075, external duct configuration, α = 10 deg and C_t = 0.6.

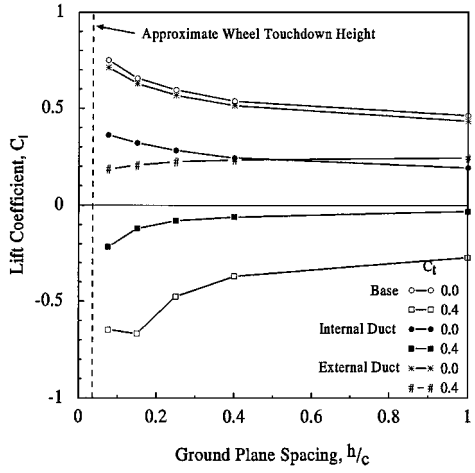

Fig. 18 Effect of ground plane spacing on lift coefficient for two-dimensional base and two exhaust ducting configurations, α = 10 deg.

Takeoff and Landing Characteristics

The takeoff and landing lift coefficient data for the base and both exhaust ducting configurations are plotted in Fig. 18. When the landing configuration data ($C_t = 0.0$) were considered, it was noted that the external duct configuration has almost identical ground effect characteristics as those for the base configuration. The internal duct configuration exhibits similar ground effect characteristics; however, it does so at greatly reduced lift coefficients. This approximately 50% reduction in lift coefficient would result in a 41% higher landing speed for the internal duct configuration. Because of this, either the base or external duct configuration appear preferable for power-off approaches and landings.

The configuration type has an even greater effect when takeoff thrust is applied. Compared to the base configuration, the internal duct configuration produced increased lift coefficients throughout all of the ground plane spacings tested. A significant advantage of this ducting scheme over the base configuration is that it exhibits much less lift coefficient dependence on thrust coefficient. This would produce an aircraft with greatly improved handling characteristics during changes in power settings, thereby enhancing safety. Despite these improvements, note that both the base and internal duct configurations produced negative lift coefficients when operating at takeoff thrust and, thus, will not lift off.

The use of the external duct configuration produced greatly improved takeoff performance when compared to either the base or internal duct configurations. Similar to the internal duct, this configuration greatly reduced the lift coefficient dependence on thrust coefficient, thereby enhancing the handling characteristics during power changes. However, the most notable advantage of this configuration is that it was the only one that produced positive lift coefficients when operated at take-off thrust levels. Based solely on these data, the external duct configuration was found to be far superior to either of the other two configurations tested.

Conclusions

Whereas the internal duct configuration did not show any significant enhancement in ground effect aerodynamic characteristics, it did show less lift coefficient dependence on thrust coefficient at the takeoff and landing angle of attack. This reduced dependence of the lift on the thrust would produce an aircraft with better takeoff characteristics and, as such, facilitate safe operation.

For the case of zero-thrust landing configurations, the base, internal and external, duct configurations had similar ground effect characteristics. However, due to a nearly 50% reduction in lift coefficient, an aircraft using the internal duct configuration would require a much higher approach and touchdown speed than one designed with the base or external ducting configurations.

The base and external duct configurations were shown to have nearly identical out-of-ground effect and ground effect characteristics at zero-thrust coefficient. However, when takeoff thrust was added, only the external duct configuration was shown to produce a positive lift coefficient. Of additional importance was that this configuration showed much less lift coefficient dependence on thrust coefficient or ground proximity when compared to the base configuration. This lack of effect would produce an aircraft with more docile characteristics than either of the other two configurations.

Based on the data acquired from this research, it was determined the external duct configuration would be the most desirable for use in a flying prototype. This conclusion was based solely on the low-speed aerodynamic characteristics of a two-dimensional model, without regard to construction considerations.

Acknowledgment

This research was supported under NASA/West Virginia University/National Aerospace Plane Grant NAG1-1584. Grant Monitor David Reubush, Hyper-X Stage Separation Manager, Hyper-X Program Office, NASA Langley Research Center.

References

[1]Gatlin, G. M., "Low-Speed Aerodynamic Characteristics of a Powered NASP-Like Configuration in Ground Effect," Society of Automotive Engineers, TP Series 892312, Sept. 1989.

[2]Gatlin, G. M., "Ground Effects on the Low-Speed Aerodynamics of a Powered, Generic Hypersonic Configuration," NASA TP 3092, 1991.

[3]Gatlin, G. M., and Kjerstad, K. J., "Low-Speed Longitudinal Aerodynamic Characteristics of a Powered National Aero-Space Plane Test Technique Demonstrator Configuration In and Out of Ground Effect," National Aerospace Plane, TP 1012, REF WBS 3.5.06, Feb. 1994.

[4]Smith, G., "Aerodynamic Coefficients of a Hypersonic NASP Model in Ground Effect," M.S. Thesis, Department of Mechanical and Aerospace Engineering, West Virginia Univ., Morgantown, WV, July 1996.

[5]Smith, G., Bond, R., Loth, J., and Morris, G., "NASP Takeoff Lift Loss Alleviation," AIAA Paper 97-0296, Jan. 1997.

[6]Romero, J. M., "Configuration Layout, NASP Display Model Version 2," Preliminary Design Drawing FW9010009A, General Dynamics, Fort Worth Div., Fort Worth, TX, Nov. 1990.

[7]Allen, H. J., and Vincenti, W. G., "Wall Interference in a Two-Dimensional Flow Wind Tunnel, with Consideration of the Effect of Compressibility," National Advisory Committee for Aeronautics, Rept. 782, 1944.